

# The effects of local fields on laser gain for layered and Maxwell Garnett composite materials

Ksenia Dolgaleva<sup>1</sup>, Robert W Boyd<sup>1</sup> and Peter W Milonni<sup>2</sup>

<sup>1</sup> The Institute of Optics, University of Rochester, Rochester, NY 14627, USA

<sup>2</sup> 104 Sierra Vista Dr, Los Alamos, NM 87544, USA

Received 14 November 2008, accepted for publication 24 November 2008

Published 14 January 2009

Online at [stacks.iop.org/JOptA/11/024002](http://stacks.iop.org/JOptA/11/024002)

## Abstract

We develop simple theoretical models for calculating the effective linear susceptibilities of layered and Maxwell Garnett composite materials with a gain resonance in one of their components. We distinguish two cases of resonant components: the case of ‘pure resonant emitters’, in which all the atoms or molecules of the resonant medium are of the same sort, and the case of ‘resonant emitters in a background’, in which only a fraction of the molecules or atoms comprising the resonant component of a composite material are in resonance with the optical field. Analysis of these models suggests that local-field effects in composite materials can provide a useful means for controlling the optical properties of laser gain media.

**Keywords:** composite optical materials, laser properties, laser gain media, local-field effects

(Some figures in this article are in colour only in the electronic version)

## 1. Introduction

Nanocomposite optical materials, which are nanoscale mixtures of two or more homogeneous materials, are becoming increasingly important in laser applications as nanofabrication technology has been rapidly developing. In particular, nanoscale ceramic composite laser gain media with improved optical properties have been reported [1, 2]. It has also been shown that one can improve the performance of a laser material by mixing it with some other material on a nanoscale in such a way that the thermal refractive index changes of the resulting composite material are smaller than those of either of the constituents [3, 4]. In the current paper we are concerned with a somewhat different approach to controlling the laser properties of nanocomposite materials: by implementing local-field effects [5, 6].

It has been previously shown that local-field effects in nanocomposite materials can lead to a large enhancement of the nonlinear optical response [7–15]. The influence of local-field effects on the linear optical properties of composite materials is not as dramatic, but certainly deserves investigation, as it can be a useful tool in controlling the laser properties of materials. We have recently shown that the basic laser properties, such as the radiative lifetime

of the upper laser level, small-signal gain coefficient, and saturation intensity, can be controlled independently by means of local-field effects [16]. In that publication, we made an approximation, treating a composite material of any geometry as a quasi-homogeneous medium characterized by an effective refractive index, with the local-field effects accounted for using the Lorentz model [5, 6]. Within that model, the local field  $\mathbf{E}_{\text{loc}}$  acting on a typical molecule or atom of a medium is related to the macroscopic average field  $\mathbf{E}$  in the medium according to the expression  $\mathbf{E}_{\text{loc}}/\mathbf{E} = (\epsilon + 2)/3$ , where  $\epsilon$  is the dielectric permittivity of the medium. The Lorentz model of the local field has been shown to be applicable to homogeneous media where only one type of atom or molecule is present [17]. However, local-field effects can manifest themselves differently in composite materials, and separate theoretical models for describing the laser properties of different composite geometries [18] are needed. In this study we report such models for layered [9, 18] and Maxwell Garnett [7, 18–20] composite geometries. One can follow the recipe that we give in the current paper to assess the laser properties of more complex composite systems as well.

In section 2 we present an overview of the Lorentz and Onsager models, which are used for describing local-field effects in homogeneous (non-composite) media. In section 3

we present the modifications to the Lorentz model for the case in which only a fraction of the atoms or molecules comprising a medium is in resonance with the applied optical field. We use the general results obtained in section 3 in the following sections. In section 4 we consider composite materials of layered geometry under the assumption that one of the constituents contains molecules or atoms that are in resonance with the optical field. We derive the complex susceptibility for such a system, from which one can deduce the absorption and gain coefficients. In the process of the derivation, we obtain a modified local-field-induced frequency shift, similar to the well-known Lorentz red shift [21] in ‘pure’ systems with only one type of molecule or atom. We perform similar calculations for the Maxwell Garnett composite geometry in section 5. In section 6 we analyze the results obtained in the previous sections, considering two physical systems corresponding to the layered and Maxwell Garnett composite geometries. We summarize our conclusions in section 7.

## 2. Local-field models for homogeneous media

It is conventional to describe local-field effects in a homogeneous material medium using the well-known Lorentz model. In the simplest version of this model, one treats the medium as a cubic lattice of point dipoles of the same sort. In order to find the local field acting on a typical dipole of the medium, one surrounds the dipole of interest with an imaginary spherical cavity of radius much larger than the distance between the dipoles, and much smaller than the optical wavelength of interest. The contributions to the local field from the dipoles situated inside the spherical cavity are accounted for exactly, while the dipoles outside the cavity are treated as uniformly distributed, characterized by some average macroscopic polarization  $\mathbf{P}$ . This approach yields the well-known expression<sup>3</sup>

$$\mathbf{E}_{\text{loc}} = \mathbf{E} + \frac{4\pi}{3}\mathbf{P} \quad (1)$$

for the local field in terms of the average macroscopic electric field  $\mathbf{E}$  and the macroscopic polarization. The details of the derivation of equation (1) are given elsewhere [5, 6, 22]. It is also convenient to express the local field as

$$\mathbf{E}_{\text{loc}} = L\mathbf{E} \quad (2)$$

in terms of the local-field correction factor

$$L = \frac{\epsilon + 2}{3}. \quad (3)$$

The other commonly used model for describing the local field in homogeneous media has been developed by Onsager [23]. In his study, Onsager treats a molecule or atom as being enclosed in a tiny *real* cavity in the medium. Then the field acting on the molecule is divided into the cavity field, which would exist at the center of the real cavity in the absence of the molecule, and the reaction field, which corrects the cavity field for the polarization of the surrounding medium by

the dipole field of the molecule in the cavity. The resulting local field is given by

$$\mathbf{E}_{\text{loc}} = \frac{3\epsilon}{2\epsilon + 1}\mathbf{E} + \frac{2(\epsilon - 1)}{(2\epsilon + 1)a^3}\mathbf{p} \quad (4)$$

with the first and second terms being the cavity and reaction field, respectively. Here  $a$  is the cavity radius, and  $\mathbf{p}$  is the dipole moment of the molecule. Even though the Lorentz and Onsager models yield different expressions for the local field, microscopic theories, developed in [17] and [24], reconcile those two models, which appear to be two special cases of the more general theories.

In reality, there is no need to apply a full microscopic treatment of local-field effects in order to describe an experimental outcome. In most cases, one of the two macroscopic theories works reasonably well. The Onsager model is applicable to polar liquids, while the Lorentz model is applicable to solids and non-polar liquids. Both models can describe a guest–host system. The Lorentz model describes such a system in cases when the guest’s molecule or atom replaces a molecule or atom of the host with similar polarizability [17]. An example is neodymium-doped YAG, where neodymium guest ions replace yttrium ions in the crystalline structure. Both neodymium and yttrium belong to the class of rare-earth metals, which implies that they have similar properties. The Onsager model is more suitable when the polarizability of a guest is significantly different from that of the host molecules or atoms. Then the guest not only forms a cavity in the host medium, but affects the local field outside the cavity [23, 25]. A good example of such a guest–host system is provided by liquid solutions of fullerene  $C_{60}$  [25].

In this paper we consider composite materials consisting of two homogeneous constituents. When studying local-field effects in more complex systems one should account for the local field in the constituents, together with the local-field modifications imposed by the geometry of the composite. Within this study, we limit ourselves to the case in which the homogeneous constituents obey the Lorentz model of the local field. One can easily extend our formalism to the case of Onsager-type constituents.

## 3. Lorentz local field in a resonant medium

We first consider a pure, homogeneous resonant medium illuminated by an optical field of frequency  $\omega$ . We assume that the field is tuned close to a resonance of the atoms. In that case we can treat the medium roughly as a collection of two-level atoms, and can apply a well-known formalism, based on the Maxwell–Bloch equations [26], to describe the optical properties of such a medium. We insert the local field into the equations for the slowly varying amplitude  $\sigma^{(1)}$  of the coherence  $\tilde{\sigma}^{(1)}(t) = \sigma^{(1)} \exp(-i\omega t) + \text{c.c.}$  and population inversion  $w$ :

$$\dot{\sigma}^{(1)} = \left( i\Delta - \frac{1}{T_2} \right) \sigma^{(1)} - \frac{1}{2} i\kappa w E_{\text{loc}}; \quad (5a)$$

$$\dot{w} = -\frac{w - w_{\text{eq}}}{T_1} + i \left( \kappa E_{\text{loc}} (\sigma^{(1)})^* - \kappa^* E_{\text{loc}}^* \sigma^{(1)} \right). \quad (5b)$$

<sup>3</sup> We use Gaussian units in this paper.

Here  $\Delta = \omega - \omega_0$  is the detuning of the optical frequency  $\omega$  from the atomic resonance frequency  $\omega_0$ ,  $T_1$  and  $T_2$  are the population and coherence relaxation times, respectively,  $w_{\text{eq}}$  is the equilibrium value of the population inversion (e.g., in the case of an uninverted system,  $w_{\text{eq}} = -1$ ), and  $\kappa = 2\mu/\hbar$ , where  $\mu$  is the dipole moment of the atomic transition. Here and below, we use a tilde to denote the time-dependent quantities, and similar variables without a tilde to denote their slowly varying amplitudes. We will only concern ourselves here with the linear optical response. The superscript ‘(1)’ is used to emphasize this.

We substitute the Lorentz local field, given by equation (1), with the average electric field in the medium  $\tilde{E}(t)$  and macroscopic polarization  $\tilde{P}(t)$  into the Maxwell–Bloch equations (5). It is convenient to express the slowly varying amplitude  $P$  in terms of the coherence, transition dipole moment, and molecular or atomic density  $N$  according to [27]

$$P = N\mu^*\sigma^{(1)}. \quad (6)$$

Substitution of equation (6) into equations (5) with the local field in the form of equation (1) results in the appearance of the inversion-dependent frequency shift,  $\Delta_L w$ , in the equation for  $\sigma^{(1)}$ ,

$$\dot{\sigma}^{(1)} = \left( i\Delta + i\Delta_L w - \frac{1}{T_2} \right) \sigma^{(1)} - \frac{1}{2} i\kappa w E, \quad (7)$$

which is a consequence of local-field effects. The quantity  $\Delta_L$  is known as the Lorentz red shift [21], and is given by

$$\Delta_L = -\frac{4\pi}{3} \frac{N|\mu|^2}{\hbar}. \quad (8)$$

The inversion-dependent frequency shift  $\Delta_L w$  involves a shift of the resonance of the atomic transition. The equation for the population inversion  $w$  retains its form upon the substitution of the local field (1), with  $E$  in place of  $E_{\text{loc}}$ .

The slowly varying amplitude  $P$  of the macroscopic polarization can be expressed in terms of the linear susceptibility  $\chi^{(1)}$  as  $P = \chi^{(1)} E$ . We find from equation (6) that

$$\chi^{(1)} = \frac{N\mu^*\sigma^{(1)}}{E}. \quad (9)$$

Substituting the steady-state solution of equation (5a) for the coherence  $\sigma^{(1)}$  yields

$$\chi^{(1)} = \frac{N|\mu|^2}{\hbar} \frac{w_{\text{eq}}}{\Delta + \Delta_L w_{\text{eq}} + i/T_2}. \quad (10)$$

Now we can find small-signal gain ( $g_0$ ) and absorption ( $\alpha_0$ ) coefficients of the medium from [16]:

$$g_0 = -\alpha_0 = -\frac{4\pi\omega}{c\sqrt{\epsilon}} \text{Im}\chi^{(1)}. \quad (11)$$

The dielectric permittivity  $\epsilon$  entering equation (11) is the effective dielectric permittivity, describing the dielectric properties of the entire material structure away from its resonances.

The above analysis is valid for the case of ‘pure resonant emitters’ (PREs) in which all atoms are of the same sort. However, when dealing with laser gain media, it is more typical to have a system with atoms or molecules of two or more sorts. Therefore, it is useful to modify the above two-level model to consider the case in which one has a background (host) material with the transition frequencies far from that of the optical field, doped with some portion of atoms with a transition frequency in resonance with the optical field. We refer to this case as ‘resonant emitters in a background’ (REBs) in this paper. For this kind of medium, we can split the total polarization entering equation (1) for the Lorentz local field (we call it  $P_{\text{tot}}$  from now on) into a contribution coming from the atoms of the background medium and a contribution from the resonant atoms:

$$P_{\text{tot}} = N_{\text{bg}} \alpha_{\text{bg}} E_{\text{loc}} + N_{\text{res}} \mu_{\text{res}}^* \sigma_{\text{res}}^{(1)}, \quad (12)$$

where  $\alpha_{\text{bg}}$  is the polarizability of a background atom. Here and below the parameters with the subscripts ‘bg’ and ‘res’ refer to the background and resonant atoms or molecules of the medium. As we consider only media in which the Lorentz model of the local field is valid, both resonant and background types of molecules or atoms should experience the same Lorentz local field.

One can relate here the polarizability  $\alpha_{\text{bg}}$  to the dielectric constant of the background material  $\epsilon_{\text{bg}}$  using the Clausius–Mossotti (or Lorentz–Lorenz) relation [6, 22, 25]

$$\frac{\epsilon_{\text{bg}} - 1}{\epsilon_{\text{bg}} + 2} = \frac{4\pi}{3} N_{\text{bg}} \alpha_{\text{bg}}. \quad (13)$$

Substituting equation (12) into equation (1) for the local field and using the Clausius–Mossotti relation (13) and equation (3) for the local-field correction factor, we find

$$E_{\text{loc}} = L_{\text{bg}} \left( E + \frac{4\pi}{3} P_{\text{res}} \right), \quad (14)$$

where  $L_{\text{bg}} = (\epsilon_{\text{bg}} + 2)/3$  is the local-field correction factor in the background medium. The expression for the local field reduces to equation (1) if one considers a vacuum to be a background medium.

Next, we find the susceptibility of the medium from the relationship  $\chi^{(1)} = P_{\text{tot}}/E$ . Substituting equation (13) into equation (12) for the total polarization, and then equation (12) and the steady-state solution for  $\sigma_{\text{res}}^{(1)}$  into the above relationship for  $\chi^{(1)}$ , we arrive at the result

$$\chi^{(1)} = \chi_{\text{bg}}^{(1)} + \frac{N_{\text{res}} |\mu_{\text{res}}|^2}{\hbar} \frac{L_{\text{bg}}^2 w_{\text{eq, res}}}{\Delta + \Delta'_L w_{\text{eq, res}} + i/T_{2, \text{res}}} \quad (15)$$

for the linear susceptibility of the REB medium. The frequency shift  $\Delta'_L$  is a modified Lorentz red shift given by

$$\Delta'_L = -\frac{4\pi}{3} \frac{N_{\text{res}} |\mu_{\text{res}}|^2}{\hbar} L_{\text{bg}} = L_{\text{bg}} \Delta_L. \quad (16)$$

This enhancement of the Lorentz red shift by  $L_{\text{bg}}$  due to the influence of the background dielectric medium had been previously noted in [28]<sup>4</sup>.

<sup>4</sup> This shift should be distinguished from another frequency shift of an atom in a host dielectric, namely the correction to the Lamb shift due to van der Waals interactions of the guest and host atoms. The latter is analyzed in [29].

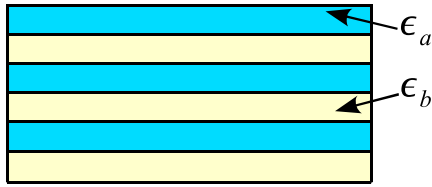


Figure 1. Layered composite material.

#### 4. Linear susceptibility of layered composite materials

Layered composite materials [9, 18] are periodic structures consisting of alternating layers of two or more homogeneous materials with different optical properties. The thicknesses of the layers should be much smaller than the optical wavelength. We will consider a layered composite material comprised of two types of homogeneous media (we call them  $a$  and  $b$ ) with different optical properties (see figure 1). Layered composite materials are anisotropic. For light polarized parallel to the layers of such a composite the effective (average) dielectric constant is given by a simple volume average of the dielectric constants of the constituents:

$$\epsilon_{\text{eff},\parallel} = f_a \epsilon_a + f_b \epsilon_b. \quad (17)$$

Here  $f_a$  and  $f_b$  are the volume fractions of the species  $a$  and  $b$ , respectively. The electric field in this case is spatially uniform, as the boundary conditions require continuity of its tangential part on the border between the two constituents. For light polarized perpendicular to the layers, the effective dielectric constant is given by

$$\frac{1}{\epsilon_{\text{eff},\perp}} = \frac{f_a}{\epsilon_a} + \frac{f_b}{\epsilon_b}. \quad (18)$$

In the latter case the electric field is non-uniformly distributed between the two constituents in the composite, and local-field effects are of particular interest. In our study we will consider the situation in which the incident electric field has a component perpendicular to the layers.

Let us assume that both components  $a$  and  $b$  of our layered composite material respond linearly to the applied optical field. Assume that the field of frequency  $\omega$  is tuned close to one of the resonances of the component  $a$ , but does not coincide with any of the resonances of the component  $b$ . We further follow the recipe given in [9] for deriving the local field in a layer  $a$ .

We choose an axis  $Z$  to be perpendicular to the layers and focus on describing the  $Z$ -component of the electric field and polarization. We define  $E$  and  $P$  to be the average macroscopic field and polarization in the composite material, respectively,  $e_a$  and  $e_b$  to denote mesoscopic fields in layers  $a$  and  $b$ , respectively,  $E_{a,\text{loc}}$  as a local field in layer  $a$ , and  $p_a$  and  $p_b$  as mesoscopic polarizations in layers  $a$  and  $b$ , respectively. For simplicity of notation, we do not write the indices  $z$ , indicating  $Z$ -components for the fields and polarizations. Following the results obtained in [9] we can write

$$e_j = E + 4\pi P - 4\pi p_j, \quad (19)$$

where  $j = a, b$ , for the mesoscopic fields in layers  $a$  and  $b$ . The macroscopic polarization is related to the mesoscopic polarizations in layers  $a$  and  $b$  as

$$P = f_a p_a + f_b p_b \quad (20)$$

with the volume fractions obeying the relationship  $f_a + f_b = 1$ . As the applied optical field's frequency does not coincide with any of the resonances of the medium  $b$ , we can simply write

$$p_b = \chi_b^{(1)} e_b \quad (21)$$

for the mesoscopic field and polarization in a layer  $b$ , with  $\chi_b^{(1)}$  denoting the linear susceptibility in the layer. Using equation (21) and the relationship  $\epsilon_b = 1 + 4\pi \chi_b^{(1)}$  for the dielectric constant and susceptibility in layer  $b$ , we obtain from equation (19) the expressions for the mesoscopic fields in terms of the average field  $E$  and the mesoscopic polarization  $p_a$  in the form

$$e_a = \frac{\epsilon_b}{1 + 4\pi f_a \chi_b^{(1)}} E - \frac{4\pi f_b}{1 + 4\pi f_a \chi_b^{(1)}} p_a \quad (22a)$$

and

$$e_b = \frac{1}{1 + 4\pi f_a \chi_b^{(1)}} E + \frac{4\pi f_a}{1 + 4\pi f_a \chi_b^{(1)}} p_a. \quad (22b)$$

Next we want to express the local field  $E_{a,\text{loc}}$  in a layer  $a$  in terms of the average field  $E$  and the mesoscopic polarization  $p_a$ . Here we distinguish two cases: the case of PREs, in which all the atoms or molecules of the material  $a$  are of the same sort, and the case of REBs, in which only some of the atoms or molecules of the homogeneous medium  $a$  are in resonance with the optical field.

##### 4.1. Case of pure resonant emitters

We first treat the simpler case of PREs in the constituent  $a$ . In this case, the local field in the medium  $a$  takes the form

$$E_{a,\text{loc}} = e_a + \frac{4\pi}{3} p_a. \quad (23)$$

Substituting equation (22a) into equation (23), we find the expression for the local field in terms of the average field and the mesoscopic polarization in a layer  $a$ ,

$$E_{a,\text{loc}} = \frac{\epsilon_b}{1 + 4\pi f_a \chi_b^{(1)}} E + \frac{4\pi}{3} \frac{f_a \epsilon_b - 2f_b}{1 + 4\pi f_a \chi_b^{(1)}} p_a. \quad (24)$$

The effective susceptibility of the layered composite material can be found from  $\chi_{\text{eff}}^{(1)} = P/E$ . Substituting  $p_b$  in the form of equation (21) and  $p_a$  in the form of equation (6) into equation (20) for the macroscopic polarization, and using equation (22b) for  $e_b$  and the steady-state solution for the coherence  $\sigma_a^{(1)}$ , we finally obtain the expression for the effective susceptibility of a layered composite material with PREs in the constituent  $a$ :

$$\chi_{\text{eff}}^{(1)} = \frac{f_a \epsilon_b^2}{(1 + 4\pi f_a \chi_b^{(1)})^2} \frac{N_a |\mu_a|^2}{\hbar} \frac{w_{\text{eq},a}}{\Delta + \Delta_1 w_{\text{eq},a} + i/T_{2,a}} + \frac{f_b \chi_b^{(1)}}{1 + 4\pi f_a \chi_b^{(1)}}. \quad (25)$$

The local-field-induced frequency shift  $\Delta_l$  of the resonance feature has the form

$$\Delta_l = -\frac{4\pi}{3} \frac{|\mu_a|^2 N_a}{\hbar} \frac{f_a \epsilon_b - 2f_b}{1 + 4\pi f_a \chi_b^{(1)}}. \quad (26)$$

The subscript ‘a’ for the atomic parameters indicates that they refer to the resonant constituent *a*. One can easily verify that in the limiting case of  $f_a \rightarrow 1$  and  $f_b \rightarrow 0$  equation (25) reduces to equation (10) for the susceptibility of a pure homogeneous medium, and equation (26) takes the form of equation (8) for the Lorentz red shift. In the opposite limiting case of  $f_a \rightarrow 0$  and  $f_b \rightarrow 1$ , the effective susceptibility reduces to  $\chi_b^{(1)}$ .

#### 4.2. Case of resonant emitters in a background

Now we consider the case of REBs in layers *a*. In that case, the local field  $E_{a,loc}$  in the layer *a* can be expressed as

$$E_{a,loc} = e_a + \frac{4\pi}{3} (p_{a,bg} + p_{a,res}). \quad (27)$$

The background and resonant contributions to the total mesoscopic polarization of the material *a* are given by

$$p_{a,bg} = N_{a,bg} \alpha_{a,bg} E_{a,loc} \quad (28a)$$

and

$$p_{a,res} = N_{a,res} \mu_{a,res}^* \sigma_{a,res}^{(1)}. \quad (28b)$$

Substituting equations (28a) and (22a) into equation (27) yields the expression for the local field in terms of the average field and the resonant contribution to the mesoscopic polarization,

$$E_{a,loc} = \frac{L_{a,bg} \epsilon_b}{1 + 4\pi (f_a \chi_b^{(1)} + f_b \chi_{a,bg}^{(1)})} E + \frac{4\pi}{3} \frac{L_{a,bg} (1 + 4\pi f_a \chi_b^{(1)} - 3f_b)}{1 + 4\pi (f_a \chi_b^{(1)} + f_b \chi_{a,bg}^{(1)})} p_{a,res}. \quad (29)$$

We find the effective susceptibility from  $\chi_{eff}^{(1)} = P/E$ , using equations (20), (21), (22b), (28), (29), and the steady-state solution for the coherence  $\sigma_{a,res}^{(1)}$ :

$$\begin{aligned} \chi_{eff}^{(1)} = & f_a \frac{\epsilon_b}{1 + 4\pi f_a \chi_b^{(1)}} \frac{\epsilon_b}{1 + 4\pi (f_a \chi_b^{(1)} + f_b \chi_{a,bg}^{(1)})} \\ & \times \left[ \chi_{a,bg}^{(1)} + L_{a,bg} \left( \frac{4\pi}{3} \frac{\chi_{a,bg}^{(1)} (1 + 4\pi f_a \chi_b^{(1)} - 3f_b)}{1 + 4\pi (f_a \chi_b^{(1)} + f_b \chi_{a,bg}^{(1)})} + 1 \right) \right. \\ & \left. \times \frac{N_{a,res} |\mu_{a,res}|^2}{\hbar} \frac{w_{eq,res}}{\Delta + \Delta'_l w_{eq,res} + i/T_{2,res}} \right] \\ & + \frac{f_b \chi_b^{(1)}}{1 + 4\pi f_a \chi_b^{(1)}}. \end{aligned} \quad (30)$$

The frequency shift  $\Delta'_l$  of the resonant feature is given by

$$\Delta'_l = -\frac{4\pi}{3} \frac{|\mu_{a,res}|^2 N_{a,res}}{\hbar} \frac{L_{a,bg} (1 + 4\pi f_a \chi_b^{(1)} - 3f_b)}{1 + 4\pi (f_a \chi_b^{(1)} + f_b \chi_{a,bg}^{(1)})}. \quad (31)$$

In the limit  $f_a \rightarrow 1$  and  $f_b \rightarrow 0$ , equation (30) reduces to equation (15), and the frequency shift (31) reduces to the

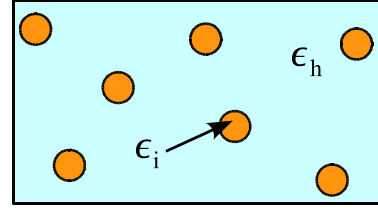


Figure 2. Maxwell Garnett composite material.

modified Lorentz red shift (16). In the opposite limiting case of  $f_a \rightarrow 0$  and  $f_b \rightarrow 1$ , we obtain  $\chi_{eff}^{(1)} = \chi_b^{(1)}$ .

### 5. Linear susceptibility of Maxwell Garnett composite materials

The Maxwell Garnett type of composite geometry is a collection of small particles (the inclusions) distributed in a host medium (see figure 2). The inclusions are assumed to be spheres of a size much smaller than the optical wavelength; the distance between them must be much larger than their characteristic size and much smaller than the optical wavelength. Under these conditions, one can treat the composite material as an effective medium, characterized by an effective (average) dielectric constant,  $\epsilon_{eff}$ , which satisfies the relation [7, 19, 20]

$$\frac{\epsilon_{eff} - \epsilon_h}{\epsilon_{eff} + 2\epsilon_h} = f_i \frac{\epsilon_i - \epsilon_h}{\epsilon_i + 2\epsilon_h}. \quad (32)$$

Here  $\epsilon_h$  and  $\epsilon_i$  are the dielectric constants of the host and inclusion materials, respectively, and  $f_i$  is the volume fraction of the inclusion material in the composite.

In this section we derive the local-field-corrected total susceptibility function for a Maxwell Garnett composite material with homogeneous host and inclusion materials. Because of the geometry of Maxwell Garnett composite materials, the local field is uniform in the inclusion medium and non-uniform in the host [7]. We limit ourselves to treating the case of resonant species in inclusions, as treating a more complicated case of resonance in a host is beyond the scope of this paper. Following our recipe, one can numerically solve the problem of deducing the total susceptibility and associated frequency shift of the resonant feature for the latter case.

Assuming that both the host and inclusion materials respond linearly to the applied optical field and following the prescriptions given in [7], we derive equation (A.8) for the mesoscopic electric field  $e_i$  in an inclusion in the appendix. Here we drop the vector notation, as the inclusion medium is assumed to be isotropic and uniform:

$$e_i = \frac{3\epsilon_h}{3\epsilon_h - 4\pi f_h \chi_h^{(1)}} \left[ E - \frac{4\pi}{3\epsilon_h} f_h p_i \right]. \quad (33)$$

In the above equation  $\chi_h^{(1)}$  and  $f_h$  are the linear susceptibility and volume fraction of the host, respectively, and  $p_i$  is the mesoscopic polarization in an inclusion. As in section 4, we consider the cases of PREs and REBs in inclusions.

### 5.1. Case of pure resonant emitters

We obtain the expression for the local field  $E_{i,\text{loc}}$  acting on the emitters in an inclusion from equation (1):

$$E_{i,\text{loc}} = e_i + \frac{4\pi}{3} p_i. \quad (34)$$

Substituting equation (33) yields

$$E_{i,\text{loc}} = \frac{3\epsilon_h}{3\epsilon_h - 4\pi f_h \chi_h^{(1)}} E + \frac{4\pi}{3} \frac{\epsilon_h(2 + f_i) - 2f_h}{3\epsilon_h - 4\pi f_h \chi_h^{(1)}} p_i. \quad (35)$$

Substituting the local field (35) into the Maxwell–Bloch equations (5), we find their steady-state solutions.

The macroscopic polarization  $P$  is an average of the mesoscopic polarization  $p(r)$ :

$$P = \int \tilde{\Delta}(r - r') p(r') dr'. \quad (36)$$

The weighting function  $\tilde{\Delta}(r)$  is defined in [7] and in the appendix. Introducing the functions

$$p(r) = \begin{cases} p_i(r) & \text{if } r \in \text{inclusion,} \\ p_h(r) & \text{if } r \in \text{host,} \end{cases} \quad (37)$$

we can represent the macroscopic polarization as an average of the mesoscopic polarizations  $p_i$  and  $p_h$  in the inclusions and host:

$$P = \int \tilde{\Delta}(r - r') p_i(r') dr' + \int \tilde{\Delta}(r - r') p_h(r') dr'. \quad (38)$$

We can represent the macroscopic electric field  $E$  as an average of the mesoscopic electric fields in the inclusion and host in a similar way. Since the mesoscopic polarization and electric field in an inclusion are uniform, the first term on the right-hand side of equation (38) is equal to  $f_i p_i$ . Similarly, one can obtain  $f_i e_i$  for the electric field. Using this result, we find the expression for the macroscopic polarization:

$$P = f_i p_i(r) + \chi_h^{(1)} E - f_i \chi_h^{(1)} e_i(r). \quad (39)$$

Substituting equation (33) for  $e_i$ , equation (6) for the resonant  $p_i$ , and the steady-state solution for  $\sigma_i^{(1)}$  into equation (39) for the macroscopic polarization, and using the relationship  $\chi_{\text{eff}}^{(1)} = P/E$ , we finally obtain the expression for the effective susceptibility of a Maxwell Garnett composite material with a resonance in the inclusions:

$$\chi_{\text{eff}}^{(1)} = f_i \left( \frac{3\epsilon_h}{3\epsilon_h - 4\pi f_h \chi_h^{(1)}} \right)^2 \frac{N_i |\mu_i|^2}{\hbar} \times \frac{w_{\text{eq},i}}{\Delta + \Delta_{\text{MG}} w_{\text{eq},i} + i/T_2} + f_h \frac{\chi_h^{(1)}(2\epsilon_h + 1)}{3\epsilon_h - 4\pi f_h \chi_h^{(1)}}. \quad (40)$$

The Maxwell Garnett frequency shift  $\Delta_{\text{MG}}$  of the resonance feature has the form

$$\Delta_{\text{MG}} = -\frac{4\pi}{3} \frac{N_i |\mu_i|^2}{\hbar} \frac{\epsilon_h(2 + f_i) - 2f_h}{3\epsilon_h - 4\pi f_h \chi_h^{(1)}}. \quad (41)$$

The subscript ‘i’ on the atomic parameters indicates that they refer to the inclusion material. It is easy to verify that equation (40) reduces to equation (10), and the frequency shift (41) reduces to the Lorentz red shift (8), in the limit  $f_i \rightarrow 1$  and  $f_h \rightarrow 0$ . We obtain  $\chi_{\text{eff}}^{(1)} = \chi_h^{(1)}$  in the opposite limiting case.

### 5.2. Case of resonant emitters in a background

Here we consider the case of REBs in inclusions. The local field  $E_{i,\text{loc}}$  acting on an emitter in an inclusion is given by equation (35) in terms of the macroscopic field  $E$  and the mesoscopic polarization  $p_i$  in an inclusion, but we need to express it in terms of the field  $E$  and the resonant part  $p_{i,\text{res}}$  of the polarization  $p_i$ , which is now

$$p_i = p_{i,\text{bg}} + p_{i,\text{res}}. \quad (42)$$

The background non-resonant and resonant contributions to the mesoscopic polarization of an inclusion are given by

$$p_{i,\text{bg}} = N_{i,\text{bg}} \alpha_{i,\text{bg}} E_{i,\text{loc}} \quad (43a)$$

and

$$p_{i,\text{res}} = N_{i,\text{res}} \mu_{i,\text{res}}^* \sigma_{i,\text{res}}^{(1)}. \quad (43b)$$

Substituting equations (42) and (43) into equation (35) yields the expression

$$E_{i,\text{loc}} = \frac{3\epsilon_h L_{i,\text{bg}}}{3\epsilon_h + 4\pi f_h (\chi_{i,\text{bg}}^{(1)} - \chi_h^{(1)})} E + \frac{4\pi}{3} L_{i,\text{bg}} \frac{\epsilon_h(2 + f_i) - 2f_h}{3\epsilon_h + 4\pi f_h (\chi_{i,\text{bg}}^{(1)} - \chi_h^{(1)})} p_{i,\text{res}} \quad (44)$$

for the local field in terms of the macroscopic field and resonant contribution to the mesoscopic polarization. Substituting the local field in the form of equation (44) into the Maxwell–Bloch equations (5), we find the steady-state solution for the coherence  $\sigma_{i,\text{res}}^{(1)}$ .

One can find the effective susceptibility from  $\chi_{\text{eff}}^{(1)} = P/E$  by substituting  $P$  from equation (39) with  $e_i$  given by equation (33) and  $p_i$  given by equations (42) and (43), and the steady-state solution for  $\sigma_{i,\text{res}}^{(1)}$ :

$$\chi_{\text{eff}}^{(1)} = f_i \frac{3\epsilon_h}{3\epsilon_h - 4\pi f_h \chi_h^{(1)}} \frac{3\epsilon_h}{3\epsilon_h + 4\pi f_h (\chi_{i,\text{bg}}^{(1)} - \chi_h^{(1)})} \times \left[ \chi_{i,\text{bg}}^{(1)} + L_{i,\text{bg}} \left( \frac{4\pi}{3} \frac{\chi_{i,\text{bg}}^{(1)} [\epsilon_h(2 + f_i) - 2f_h]}{3\epsilon_h + 4\pi f_h (\chi_{i,\text{bg}}^{(1)} - \chi_h^{(1)})} + 1 \right) \right] \times \frac{N_{i,\text{res}} |\mu_{i,\text{res}}|^2}{\hbar} \frac{w_{\text{eq},\text{res}}}{\Delta + \Delta'_{\text{MG}} w_{\text{eq},\text{res}} + i/T_{2,\text{res}}} + f_h \chi_h^{(1)} \frac{2\epsilon_h + 1}{3\epsilon_h - 4\pi f_h \chi_h^{(1)}}. \quad (45)$$

The frequency shift  $\Delta'_{\text{MG}}$  is given by

$$\Delta'_{\text{MG}} = -\frac{4\pi}{3} \frac{N_{i,\text{res}} |\mu_{i,\text{res}}|^2}{\hbar} \frac{L_{i,\text{bg}} [\epsilon_h(2 + f_i) - 2f_h]}{3\epsilon_h + 4\pi f_h (\chi_{i,\text{bg}}^{(1)} - \chi_h^{(1)})}. \quad (46)$$

In the limit  $f_i \rightarrow 1$  and  $f_h \rightarrow 0$ , equation (45) reduces to equation (15), and the frequency shift (46) reduces to the modified Lorentz red shift (16). In the opposite limit,  $\chi_{\text{eff}}^{(1)} = \chi_b^{(1)}$ .

## 6. Analysis

In this section we analyze the results for the effective linear susceptibility obtained in the previous sections for the layered and Maxwell Garnett composite materials.

### 6.1. Layered geometry

The local-field-corrected effective linear susceptibility for a layered composite material with the resonance in the layers  $a$  is given by equation (25) for the case in which all the atoms or molecules of  $a$  are of the same sort (PRE case), and by equation (30) for the case in which the component  $a$  consists of particles of different sorts (REB case). One can find the small-signal gain coefficient of the layered composite material by substituting an expression for the effective susceptibility into equation (11).

Here we analyze the behavior of the small-signal gain as a function of various parameters, choosing a Rhodamine 6G-doped PMMA laser gain medium as the resonant species  $a$  in our layered composite material. The parameters of the gain medium that we used for our analysis are the emission peak wavelength  $\lambda_0 = 590$  nm, the transverse relaxation time  $T_2 = 100$  fs, the transition cross section  $\sigma_{tr} = 2 \times 10^{-16}$  cm<sup>2</sup>, the Rhodamine molecular concentration  $N = 1.8 \times 10^{18}$  cm<sup>-3</sup>, and the refractive index of PMMA,  $n_{bg} = 1.4953$ . We take the component  $b$  to be an unspecified material and vary its refractive index to see how it affects the optical response of Rhodamine-doped PMMA.

Rhodamine-doped PMMA is an example of the REB case, and, therefore, one should use equation (30) in order to describe the effective susceptibility of the system with Rhodamine-doped PMMA resonant layers. We compare the model given by equation (30) to the case of PREs, described by equation (25), in order to test whether one can use the latter approximation in case of REBs. Using the PRE model in this physical case implies that we neglect the presence of PMMA, assuming that the Rhodamine molecules are sitting in a vacuum.

We also find it informative to compare the results given by the more precise REB model (30) to that of the simplified model that we proposed in our earlier publication (see equation (40b) in [16]). The approximation underlying the simplified model is that a composite laser gain medium is represented as a quasi-homogeneous medium characterized by an effective refractive index, and the local-field effects are accounted for by the Lorentz model for homogeneous media. For the purpose of comparison, we adapt this simplified model to our REB case in the following way. We take the expression (15) for the linear susceptibility of a medium with REBs, substituting  $\chi_{eff}^{(1)}$ , deduced from equation (18) for  $\epsilon_{eff}$  of a layered composite material, in place of  $\chi_{bg}^{(1)}$ , and  $L_{eff} = (\epsilon_{eff} + 2)/3$  in place of  $L_{bg}$ . We also multiply the atomic densities appearing in the expression by the fill fraction  $f_a$  to take into account the fact that, by changing the fill fraction of the resonant component, we change the density of the resonant molecules. Then we substitute the resulting expression for  $\chi^{(1)}$  to equation (11) to find the small-signal gain coefficient, corresponding to the simplified model.

Setting the equilibrium value of the population inversion  $w_{eq} = 1$ , which corresponds to a fully inverted amplifying system, and the detuning of the optical field with respect to the resonance  $\Delta = 0$ , we plot the small-signal gain calculated using the effective susceptibility given by equation (30) as a function of the refractive index of the non-resonant component

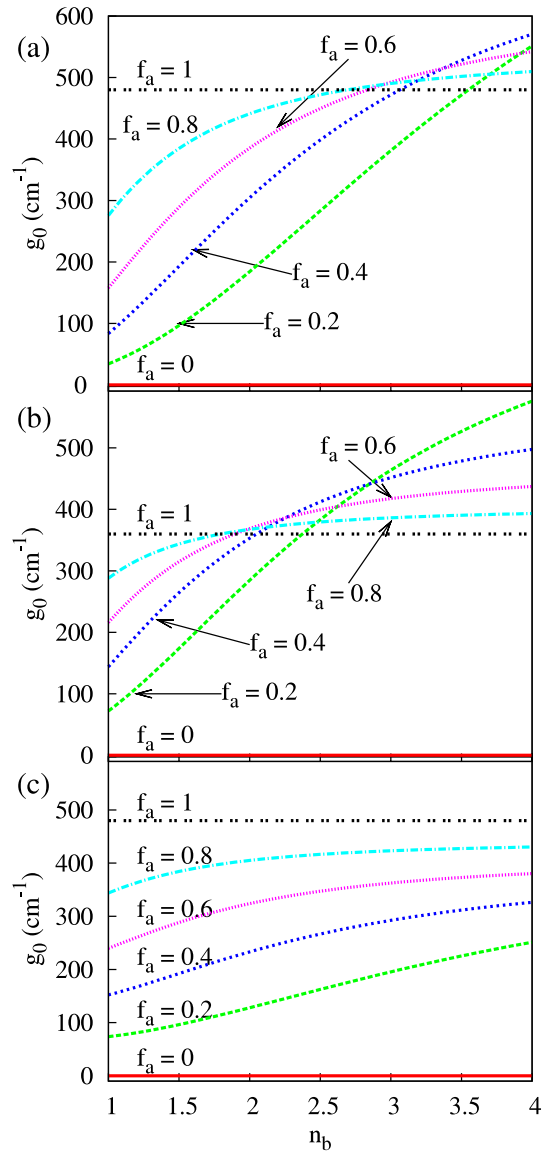


**Figure 3.** Small-signal gain of a layered composite material as a function of the refractive index of the non-resonant component for different values of the fill fraction of the resonant component: (a) REB case (derived from equation (30)), (b) PRE case (from equation (25)), (c) a simplified model from [16].

$n_b$  in figure 3(a), and of  $f_a$  in figure 4. In addition, we plot the gain coefficients derived from equation (25) and from the simplified model of [16] as functions of  $n_b$  in figures 3(b) and (c), respectively. The comparison between parts (a) and (b) of figure 3 indicates that the results for the cases of PREs and REBs differ significantly, which means that the approximation based on the assumption that all the atoms or molecules of the resonant species are of the same sort does not work in the REB case. The comparison of figures 3(a) and (c) shows moreover that the simplified model is insufficiently precise. Therefore, as we stated earlier [16], it is only good enough for a proof-of-principle study, and separate, more precise models for each composite geometry are required for an accurate description of the optical response.

It can be seen from figures 3 and 4 that the gain coefficient tends to grow with the increase of the refractive index of the

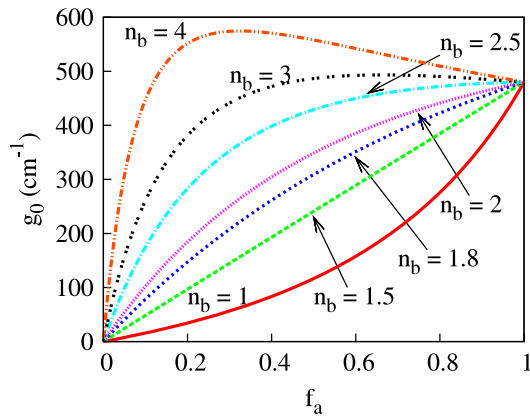


**Figure 4.** Small-signal gain of a layered composite material as a function of the fill fraction of the resonant component for different values of the refractive index of the non-resonant component. The gain is derived from equation (30) for the REB case.

non-resonant component. The reason for this behavior is that the electric field tends to localize in the regions of a dielectric with lower refractive index [9]. Therefore, the higher the refractive index of the non-resonant layers is, the more the electric field is displaced into the resonant layers, which causes a stronger gain. The behavior of the gain coefficient as a function of  $f_a$  is more complex. It grows monotonically with the increase of  $f_a$  for small refractive indices. In the case  $n_b = n_{bg}$  the growth is linear. For high values of the refractive index the small-signal gain displays a rapid growth with the increase of the fill fraction until it reaches a maximum value, corresponding to an optimal value of  $f_a$ , after which it starts to decrease with further increase of  $f_a$ . This behavior can be understood as follows. The initial growth of  $g_0$  with  $f_a$  is due to the fact that the number of resonant molecules in the medium increases. On the other hand, by increasing  $f_a$ , we make our layers with the resonant molecules thicker, and the local field, highly concentrated in these layers because of the high value of  $n_b$ , spreads over the layers, and each individual molecule ‘feels’ a smaller value of the local field. This causes the gain to decrease with the increase of  $f_a$  beyond an optimal value. Thus, in order to achieve maximum gain or absorption in a layered composite material, one needs to use a non-resonant component with a high refractive index, while keeping the fill fraction of the resonant component low.

Setting  $f_a = 0.5$  and  $n_b = 1.8$ , we plot in figure 5 the small-signal gain for REBs in the component  $a$  as a function of the frequency detuning  $\Delta$  of the optical field with respect to the molecular resonance for different values of  $w_{eq}$ . Variation of the population inversion from  $w_{eq} = -1$ , corresponding to an uninverted system, to  $w_{eq} = 1$ , describing a fully inverted system, clearly shows how the composite medium changes from an absorber to an amplifier. In reality, it is not possible to achieve a full inversion, so most physical cases correspond to  $w_{eq} < 0.5$ .

### 6.2. Maxwell Garnett geometry

The effective linear susceptibility for the Maxwell Garnett composite geometry for the cases of PREs and REBs in

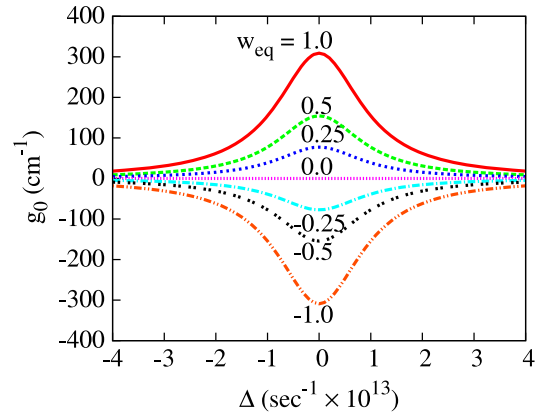


**Figure 5.** Small-signal gain of a layered composite material as a function of the detuning of the optical field with respect to the molecular resonant frequency. Marked on the graphs are the values of equilibrium population inversion.

inclusions is given by equations (40) and (45), respectively. Substituting these expressions into equation (11), we obtain the small-signal gain coefficients for the cases of PREs and REBs.

We take for our analysis a Maxwell Garnett composite material with Nd:YAG nanoparticles as inclusions. We use the emission wavelength  $\lambda_0 = 1.064 \mu\text{m}$ , the transverse relaxation time  $T_2 = 3 \text{ ms}$ , the transition cross section  $\sigma_{tr} = 4.6 \times 10^{-19} \text{ cm}^2$ , the neodymium atomic concentration  $N = 1.37 \times 10^{20} \text{ cm}^{-3}$  (this value corresponds to 1 at.% of Nd in YAG), and the YAG refractive index  $n_{bg} = 1.82$ . We take the host to be an unspecified medium, and vary its refractive index  $n_h$  to see how it affects the optical response of Nd:YAG nanoparticles.

Nd:YAG corresponds to the case of REBs, which means that the effective susceptibility of the Maxwell Garnett composite material with Nd:YAG inclusions obeys equation (45). As in section 5, we compare the small-signal gain coefficients, corresponding to the REB model, given by equation (45), to the PRE model, given by equation (40), and to the simplified model from [16], adapted to our case, in order to test the applicability of the latter two approximations. The simplified model is derived from equation (15) with  $\chi_{eff}^{(1)}$  and  $L_{eff}$ , deduced from equation (32) for  $\epsilon_{eff}$  of the Maxwell Garnett composite material, in place of  $\chi_{bg}^{(1)}$  and  $L_{bg}$ . In addition, we multiply the atomic density in the resulting equation by the inclusion fill fraction  $f_i$  in order to account for its change with the change of  $f_i$ . Then we substitute the resulting expression for  $\chi^{(1)}$  into equation (11) to deduce the gain coefficient.

Setting the equilibrium value of the population inversion  $w_{eq} = 1$  and the detuning  $\Delta = 0$ , we plot the small-signal gain coefficients derived from the REB (equation (45)) and PRE (equation (40)) models, and from the simplified model, as functions of the refractive index of the host  $n_h$  in figures 6(a), (b), and (c), respectively. The dependence of  $g_0$ , derived from equation (45), on the inclusion fill fraction  $f_i$  is depicted in figure 7. A comparison of part (a) with parts (b) and (c) of figure 6 suggests that, as in the case of the layered composite geometry, the PRE approximation and simplified

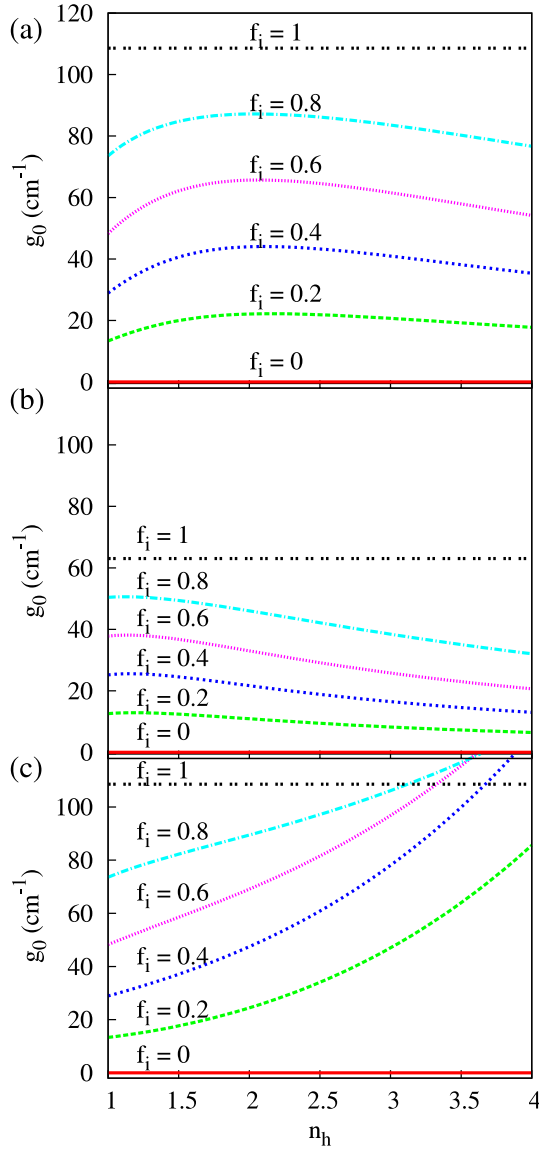


**Figure 6.** Small-signal gain of the Maxwell Garnett composite material as a function of the refractive index of the non-resonant host for different values of the inclusion fill fraction: (a) REB case (from equation (45)), (b) PRE case (from equation (40)), (c) a simplified model from [16].

model do not agree with the more precise description of the Maxwell Garnett composite material with REBs in inclusions.

One can see from figures 6 and 7 that the small-signal gain of the Maxwell Garnett composite geometry exhibits a monotonic growth with the increase of  $f_i$ . It increases to some maximum value with the increase of the host refractive index, and then decreases with further growth of  $n_h$ . The monotonic growth of  $g_0$  with  $f_i$  is due to the fact that, unlike in layered composite materials, the increase of the inclusion fill fraction in the Maxwell Garnett composite material is not accompanied by the decrease in the local field in an inclusion. The reason for the complex behavior of  $g_0$  as a function of  $n_h$  is as follows. It is seen from equation (11) that  $g_0 \propto [\sqrt{\epsilon_{\text{eff}}}]^{-1} \text{Im} \chi_{\text{eff}}^{(1)}$ . Due to the electric field localization in the component with the lower refractive index,  $\text{Im} \chi_{\text{eff}}^{(1)}$  grows monotonically with the increase

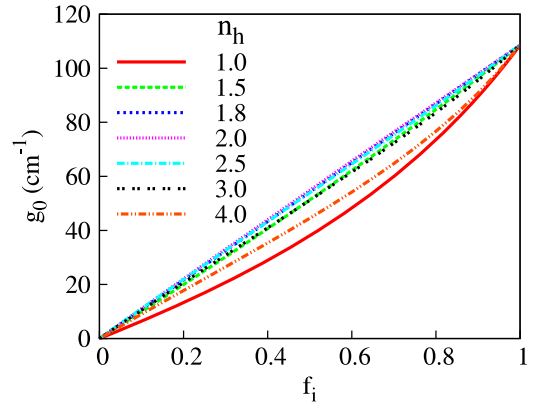


**Figure 7.** Small-signal gain of the Maxwell Garnett composite material as a function of the inclusion fill fraction for different values of the host refractive index.  $g_0$  is derived from equation (45) for the REB case.

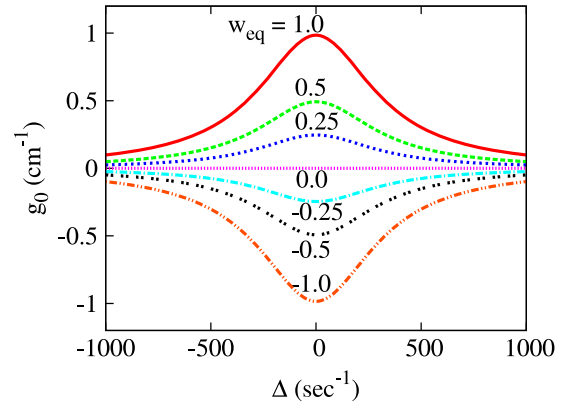


**Figure 8.** Small-signal gain of the Maxwell Garnett composite material as a function of the detuning of the optical field with respect to the molecular resonant frequency. Marked on the graphs are the values of equilibrium population inversion.

of  $n_h$ . However, the term  $[\sqrt{\epsilon_{\text{eff}}}]^{-1}$ , where  $\epsilon_{\text{eff}}$  is given by equation (32), decreases with the increase of  $n_h$ , and at some value of the host refractive index its decrease overcompensates the growth of  $\text{Im} \chi_{\text{eff}}^{(1)}$ . As a result,  $g_0$  starts to decrease with further increase of  $n_h$ .

It is important to keep in mind that the Maxwell Garnett model works well only for low fill fractions of the inclusions ( $f_i \lesssim 0.5$ ). It does not account for a percolation phenomenon that occurs when  $f_i$  is higher than a certain value.

In figure 8 we plot the small-signal gain coefficient as a function of the detuning  $\Delta$  for different values of the equilibrium population inversion  $w_{\text{eq}}$  with the fixed values  $f_i = 0.01$  and  $n_h = 1.3$ . As in the case of the layered composite geometry, one can see the change from absorption to amplification as  $w_{\text{eq}}$  changes from  $-1$  to  $1$ .

## 7. Conclusions

In this article we have developed theoretical models describing the effective linear susceptibility of layered and Maxwell Garnett composite materials with resonant components of two

types. The first type is a simple case of a resonant medium in which all the molecules or atoms are of the same sort (we call this the case of ‘pure resonant emitters’, or PREs). The second type of resonant component corresponds to a situation in which only a fraction of the molecules or atoms of the medium are in resonance with the optical field (we call this the case of ‘resonant emitters in a background’, or REBs). The latter model is more realistic, as most laser gain media consist of species of different sorts. Along the way, we derived the expressions for the frequency shifts of the resonant features with respect to the actual resonances, which are the analogs of the famous Lorentz red shift in a homogeneous medium. These frequency shifts for the layered and Maxwell Garnett composite geometries with PRE and REB components differ from the Lorentz red shift and from each other.

We analyzed the theoretically obtained expressions for the effective susceptibilities for the following two physical cases. The first case is a layered composite material with the resonant component consisting of Rhodamine-doped PMMA. The second case is a Maxwell Garnett composite material with Nd:YAG nanoparticles as resonant inclusions. Plotting the small-signal gain coefficients of the composite materials as functions of the resonant component fill fraction and the refractive index of the non-resonant component, we observed the following behavior. The gain coefficient of the linear composite geometry displayed a monotonic growth with the increase of the refractive index. Plotting the gain coefficient of the layered composite material as a function of the resonant component fill fraction, we observed a more interesting and complex behavior: the gain coefficient displayed a growth up to a certain maximum value, and then a decrease with the increase of the fill fraction of the resonant component. It appears that one can achieve a maximal gain or absorption with a layered composite geometry, taking a non-resonant component with a high refractive index, while keeping the fill fraction of the resonant component low. The small-signal gain coefficient of the Maxwell Garnett composite material exhibited a monotonic growth with the increase of the resonant component fill fraction, and went through a maximum as a function of the refractive index of the non-resonant component. The layered geometry seems to be more promising for tailoring the optical properties of the composite laser gain media: under certain conditions the gain coefficient of the layered composite geometry can exceed the gain coefficients of its constituents.

We believe that the theoretical study that we performed in this paper will be helpful in designing composite laser gain media with controlled optical properties.

### Acknowledgment

This work was supported by NSF grant ECCS-0701585.

### Appendix. Mesoscopic field in an inclusion of a Maxwell Garnett composite material

In this appendix we derive the expression for the mesoscopic field in an inclusion of a Maxwell Garnett composite material. As a starting point, we use the result for the mesoscopic field

$\mathbf{e}(\mathbf{r})$  at any point  $\mathbf{r}$  of a Maxwell Garnett composite, obtained in [7] (equation (3.8)):

$$\mathbf{e}(\mathbf{r}) = \mathbf{E}(\mathbf{r}) + \int \overset{\leftrightarrow}{\mathbf{T}}(\mathbf{r} - \mathbf{r}') \mathbf{p}'(\mathbf{r}') d\mathbf{r}' + \frac{4\pi}{3\epsilon_h} [\mathbf{P}'(\mathbf{r}) - \mathbf{p}'(\mathbf{r})]. \quad (\text{A.1})$$

Here  $\overset{\leftrightarrow}{\mathbf{T}}(\mathbf{r})$  designates a static dipole–dipole coupling tensor for a host medium with dielectric constant  $\epsilon_h$ . The mesoscopic polarization  $\mathbf{p}'(\mathbf{r})$  is a linear part of the source polarization defined in [7] (we will refer to it as the linear source polarization). It is defined as

$$\mathbf{p}'(\mathbf{r}) = \begin{cases} (\chi_i^{(1)} - \chi_h^{(1)})\mathbf{e}(\mathbf{r}), & \text{if } r \in \text{inclusion,} \\ 0, & \text{if } r \in \text{host.} \end{cases} \quad (\text{A.2})$$

Here  $\chi_i^{(1)}$  and  $\chi_h^{(1)}$  are the susceptibilities of the inclusion and host media, respectively. In this paper we are not concerned with the nonlinear interactions, so we do not consider the nonlinear part of the source polarization. The macroscopic linear source polarization  $\mathbf{P}'(\mathbf{r})$  is obtained by averaging  $\mathbf{p}'(\mathbf{r})$ ,

$$\mathbf{P}'(\mathbf{r}) = \int \tilde{\Delta}(\mathbf{r} - \mathbf{r}') \mathbf{p}'(\mathbf{r}') d\mathbf{r}', \quad (\text{A.3})$$

where  $\tilde{\Delta}(\mathbf{r})$  is a smoothly varying weighting function which has a range  $R$  much smaller than the wavelength of light, but much larger than a typical separation distance between the inclusions. The weighting function is normalized to unity:

$$\int \tilde{\Delta}(\mathbf{r} - \mathbf{r}') d\mathbf{r}' = 1. \quad (\text{A.4})$$

We are considering the mesoscopic field in an inclusion of the Maxwell Garnett composite material. In the case of an isotropic and uniform inclusion material one can assume that the polarization  $\mathbf{p}'(\mathbf{r})$  and the electric field  $\mathbf{e}(\mathbf{r})$  are mesoscopically uniform over an inclusion. Based on the above assumption and on the mathematical arguments given in [7], we can set the term involving the dipole–dipole coupling tensor in equation (A.1) equal to zero. This brings us to the expression

$$\mathbf{e}_i(\mathbf{r}) = \mathbf{E}(\mathbf{r}) + \frac{4\pi}{3\epsilon_h} [\mathbf{P}'(\mathbf{r}) - \mathbf{p}'(\mathbf{r})] \quad (\text{A.5})$$

for the mesoscopic field in an inclusion. We can find the macroscopic average polarization  $\mathbf{P}'(\mathbf{r})$  from equation (A.3), using the assumption that  $\mathbf{p}'(\mathbf{r})$  is mesoscopically uniform over an inclusion:

$$\mathbf{P}'(\mathbf{r}) = f_i \mathbf{p}'(\mathbf{r}). \quad (\text{A.6})$$

Here  $f_i$  is the volume fraction of the inclusions in the composite material. Using equation (A.2), we can express the mesoscopic polarization  $\mathbf{p}_i(\mathbf{r})$  in an inclusion as

$$\mathbf{p}_i(\mathbf{r}) = \chi_h^{(1)} \mathbf{e}_i(\mathbf{r}) + \mathbf{p}'(\mathbf{r}). \quad (\text{A.7})$$

Substituting equations (A.6) and (A.7) into equation (A.5) and making use of the relation  $f_h + f_i = 1$  for the volume fractions of the host and inclusion materials, we obtain the expression

$$\mathbf{e}_i(\mathbf{r}) = \frac{3\epsilon_h}{3\epsilon_h - 4\pi f_h \chi_h^{(1)}} \left[ \mathbf{E}(\mathbf{r}) - \frac{4\pi}{3\epsilon_h} f_h \mathbf{p}_i(\mathbf{r}) \right] \quad (\text{A.8})$$

for the mesoscopic field in an inclusion.

## References

- [1] Ikesue A and Aung Y L 2006 Synthesis and performance of advanced ceramic lasers *J. Am. Ceram. Soc.* **89** 1936–44
- [2] Basiev T T, Doroshenko M E, Konyushkin V A, Osiko V V, Ivanov L I and Simakov S V 2007 Lasing in diode-pumped fluoride nanostructure  $F_2^-$ :LiF colour centre ceramics *Quantum Electron.* **37** 989–90
- [3] Duarte F J and James R O 2003 Tunable solid-state lasers incorporating dye-doped, polymer-nanoparticle gain media *Opt. Lett.* **28** 2088–90
- [4] Duarte F J and James R O 2004 Spatial structure of dye-doped polymer nanoparticle laser media *Appl. Opt.* **43** 4088–90
- [5] Lorentz H A 1916 *Theory of Electrons* 2nd edn (Leipzig: Teubner)
- [6] Jackson J D 1999 *Classical Electrodynamics* 3rd edn (New York: Wiley)
- [7] Sipe J E and Boyd R W 1992 Nonlinear susceptibility of composite optical materials in the Maxwell Garnett model *Phys. Rev. A* **46** 1614–29
- [8] Sipe J E and Boyd R W 2002 Nanocomposite materials for nonlinear optics based on local field effects *Optical Properties of Nanostructured Random Media (Topics Appl. Phys.)* vol 82, ed V M Shalaev (Berlin: Springer) pp 1–19
- [9] Boyd R W and Sipe J E 1994 Nonlinear optical susceptibilities of layered composite materials *J. Opt. Soc. Am. B* **11** 297–303
- [10] Neeves A E and Birnboim M H 1988 Composite structures for the enhancement of nonlinear optical materials *Opt. Lett.* **13** 1087–9
- [11] Neeves A E and Birnboim M H 1989 Composite structures for the enhancement of nonlinear-optical susceptibility *J. Opt. Soc. Am. B* **6** 787–96
- [12] Fischer G L, Boyd R W, Gehr R J, Jenekhe S A, Osaheni J A, Sipe J E and Weller-Brophy L A 1995 Enhanced nonlinear optical response of composite materials *Phys. Rev. Lett.* **74** 1871–4
- [13] Smith D D, Fischer G, Boyd R W and Gregory D A 1997 Cancellation of photoinduced absorption in metal nanoparticle composites through a counterintuitive consequence of local field effects *J. Opt. Soc. Am. B* **14** 1625–31
- [14] Nelson R L and Boyd R W 1999 Enhanced electro-optic response of layered composite materials *Appl. Phys. Lett.* **74** 2417–9
- [15] Gehr R J, Fischer G L and Boyd R W 1997 Nonlinear-optical response of porous-glass-based composite materials *J. Opt. Soc. Am. B* **14** 2310–4
- [16] Dolgaleva K and Boyd R W 2007 Laser gain media based on nanocomposite materials *J. Opt. Soc. Am. B* **24** A19–25
- [17] de Vries P and Lagendijk A 1998 Resonant scattering and spontaneous emission in dielectrics: microscopic derivation of local-field effects *Phys. Rev. Lett.* **81** 1381–4
- [18] Gehr R J and Boyd R W 1996 Optical properties of nanocomposite optical materials *Chem. Mater.* **8** 1807–19
- [19] Maxwell Garnett J C 1904 Colours in metal glasses and in metallic films *Phil. Trans. R. Soc. A* **203** 385–420
- [20] Maxwell Garnett J C 1906 Colours in metal glasses, in metallic films, and in metallic solutions *Phil. Trans. R. Soc. A* **205** 237–88
- [21] Maki J J, Malcuit M S, Sipe J E and Boyd R W 1991 Linear and nonlinear optical measurements of the Lorentz local field *Phys. Rev. Lett.* **67** 972–5
- [22] Aspnes D E 1982 Local-field effects and effective-medium theory: a microscopic perspective *Am. J. Phys.* **50** 704–9
- [23] Onsager L 1936 Electric moments of molecules in liquids *J. Am. Chem. Soc.* **58** 1486–93
- [24] Hynne F and Bullough R K 1972 The Onsager reaction field as a screened self-interaction in refractive-index theory *J. Phys. A: Gen. Phys.* **5** 1272–95
- [25] Andersen J U and Bonderup E 2000 Local field corrections for light absorption by fullerenes *Eur. Phys. J. D* **11** 435–48
- [26] Hopf F A, Bowden C M and Louisell W H 1984 Mirrorless optical bistability with the use of the local-field correction *Phys. Rev. A* **29** 2591–6
- [27] Boyd R W 2003 *Nonlinear Optics* 2nd edn (New York: Academic)
- [28] Manassah J T and Gross B 1998 Amplification by an optically dense resonant two-level system embedded in a dielectric medium *Opt. Commun.* **155** 213–22
- [29] Milonni P W, Schaden M and Spruch L 1999 Lamb shift of an atom in a dielectric medium *Phys. Rev. A* **59** 4259